Supplementary information for

"Detailed electronic structure of a high-spin cobalt(II) complex determined from NMR and THz-EPR spectroscopy"

by Alexander A. Pavlov, Joscha Nehrkorn, Yanina A. Pankratova, Mykhaylo Ozerov, Elena A. Mikhalyova, Alexander V. Polezhaev, Yulia V. Nelyubina, and Valentin V. Novikov

1. Synthesis

Thallium tris(pyrazolyl)borate (**TlTp**) was obtained by two step procedure. Firstly potassium tris(pyrazolyl)borate (**NaTp**) was obtained using the literature procedure [1]. On the second step **NaTp** was converted to **TlTp** as described in [2].

CoTp$_2$ was obtained using modified literature procedure [3]. Briefly, **TlTp** and CoCl$_2$*6H$_2$O in 2:1 molar ratio were mixed in MeCN and stirred for 2 h at r.t. Volatiles were removed under vacuum and a solid residue was treated with toluene. The white precipitate of TlCl was separated and toluene was removed under vacuum yielding the target compound as light-yellow powder in quantitative yield. Analytical data were in agreement with the literature.

2. Quantum chemical calculations

All quantum chemical calculations were done using the ORCA package, v. 4.0 [4]. Molecular geometry from a previous X-ray diffraction study of **CoTp$_2$** [5] was used as a starting point for geometry optimization with the hybrid PBE0 functional, the scalar relativistic zero-order regular approximation (ZORA) [6], Grimme's DFT-D3 dispersion correction [7] and the scalar relativistically recontracted (SARC) [8] version of the def2-TZVP basis set [9]. Extra tight thresholds for forces and displacements were used. The solvation effects were included using the Conductor-like Polarizable Continuum Model, as implemented in ORCA 4.0, with toluene as a solvent. The resulting geometry was used to compute g-tensor and isotropic values of hyperfine interaction tensors A$_{iso}$ [10].

3. NMR spectroscopy

3.1. Data collection ^{1}H, ^{13}C{^{1}H}, ^{11}B{^{1}H} spectra were recorded from solutions of **CoTp$_2$** in d$_8$-toluene with a Bruker Avance 400 and 600 spectrometers, using following parameters: ^{1}H spectra: sweep width 1000 ppm, acquisition time 0.2 s, relaxation delay 0.2 s, pulse duration 6.5 μs, pulse program "zg" within Bruker notation, number of scans 1024, line-broadening factor 3 Hz; ^{13}C{^{1}H} spectra: sweep width 2000 ppm, acquisition time 0.2 s, relaxation delay 0.2 s, pulse duration

9 μs, pulse program "zgpg30" within Bruker notation, number of scans >32k, line-broadening factor 10 Hz; ^{11}B{^{1}H} spectra: sweep width 1000 ppm, acquisition time 0.1 s, relaxation delay 0.1 s, pulse duration 10 μs, pulse program "zgpg30" within Bruker notation, number of scans 1024, line-broadening factor 10 Hz. Measurements were done and the acquired spectra were calibrated using the residual signals of CD$_3$CN (^{1}H 2.09 ppm, ^{13}C 20.40 ppm). ^{11}B{^{1}H} spectrum was referenced by external 15% BF$_3$.OEt$_2$ in CDCl$_3$.

3.2. Analysis of paramagnetic shifts in NMR spectra

For the paramagnetic complex **CoTp$_2$**, the observed chemical shifts of its nuclei include diamagnetic (δ_{DIA}), contact (δ_{CS}) and pseudocontact (δ_{PCS}) contributions:

$$\delta_{OBS} = \delta_{DIA} + \delta_{CS} + \delta_{PCS} \qquad (S1)$$

As a diamagnetic contribution, chemical shifts in ^{1}H NMR spectra of the ligand, hydrotris-(1-pyrazolyl)borate [11], and in ^{13}C and ^{11}B NMR spectra of sodium trispyrazolylborate [12] were used.

Contact contribution to the chemical shifts in the NMR spectra of **CoTp$_2$** were calculated using the following equation:

$$\delta_{CS} = \frac{S(S + 1)\mu_B}{3kTg_N\mu_N} \cdot \bar{g} \cdot A_{iso} \qquad (S2)$$

where A_{iso} is a DFT-calculated isotropic hyperfine coupling constant, $\bar{g}$ **is a** DFT-calculated rotationally averaged electronic g-value, g_N is the nuclear g-value, μ_B and μ_N are the Bohr and nuclear magnetons, respectively, and kT is the thermal energy.

Pseudocontact shifts in the NMR spectra of a paramagnetic compound can be obtained according to:

$$\delta_{PCS} = \frac{1}{12\pi r^3}\left[\Delta\chi_{ax}(3cos^2\theta - 1)\right] \qquad (S3)$$

where $\Delta\chi_{ax}$ is the axial anisotropy of the magnetic susceptibility tensor (χ–tensor). The polar coordinates of nuclei r and θ were taken from a DFT-optimized geometry of **CoTp$_2$**; r –distance between the cobalt(II) ion and the nucleus of interest, θ – angle between the boron atom, the cobalt(II) ion (angle vertex) and the nucleus of interest.

For **CoTp$_2$**, the value of $\Delta\chi_{ax}$ was estimated by fitting the chemical shifts observed in the experimental ^{1}H NMR spectra to those calculated by the following equation:

$$\delta_{OBS} = \delta_{DIA} + \delta_{CS} + \frac{1}{12\pi r^3}\left[\Delta\chi_{ax}(3cos^2\theta - 1)\right] \qquad \text{(S4)}$$

4. THz-EPR spectroscopy

THz-EPR spectra were measured at the NHMFL (Tallahassee, FL). The experimental setup is described elsewhere.[13]

Transmission was measured in Voigt geometry with a Si bolometer. The sample was in thermal equilibrium with the liquid Helium bath of the 17 T split coil superconducting magnet, i.e. sample temperature was always 4.2 K. Experimental resolution was 0.8 cm^{-1}, at a scanner velocity of 10 kHz with a Mylar multilayer beam splitter.

5. Supplementary figures and schemes
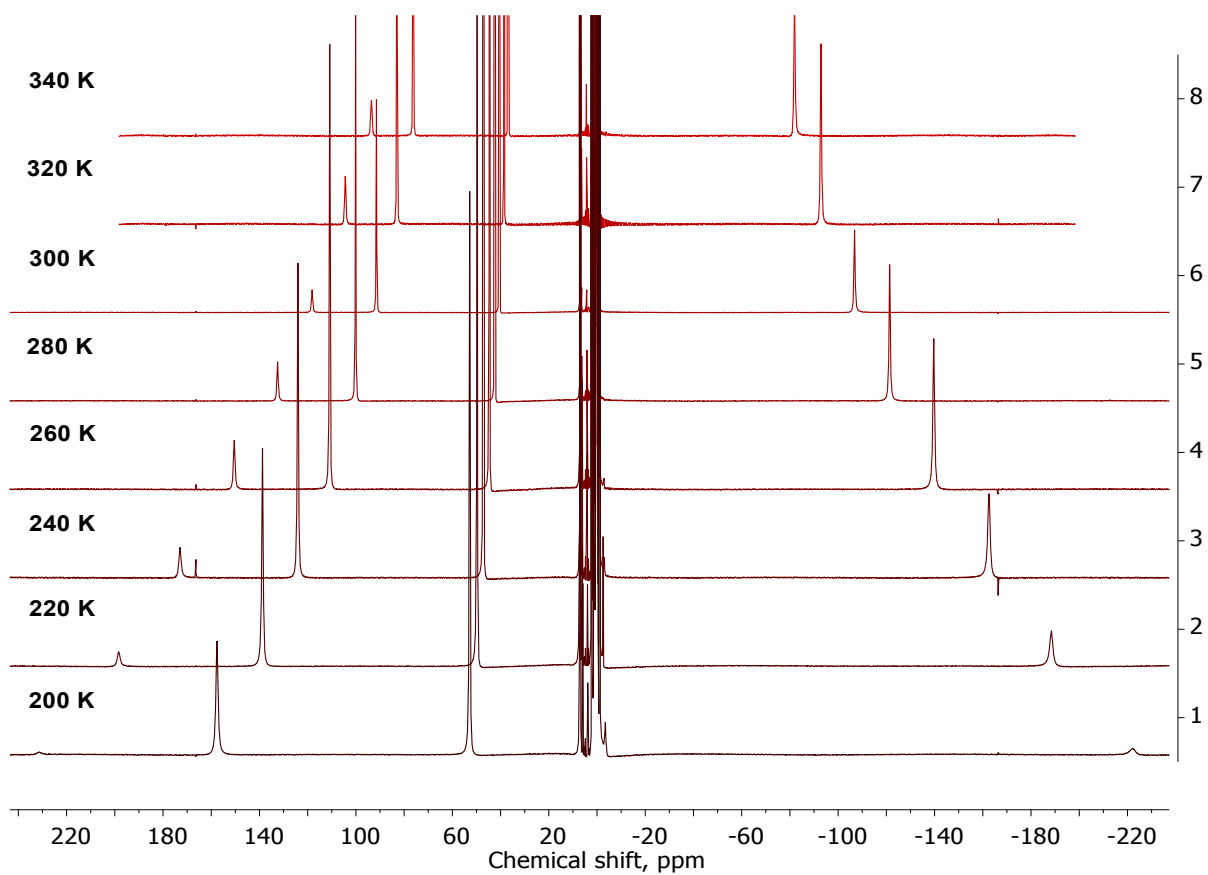
Figure S1. Temperature-dependent ^1H NMR spectra of **CoTp₂** in d$_8$-toluene (600.22 MHz).
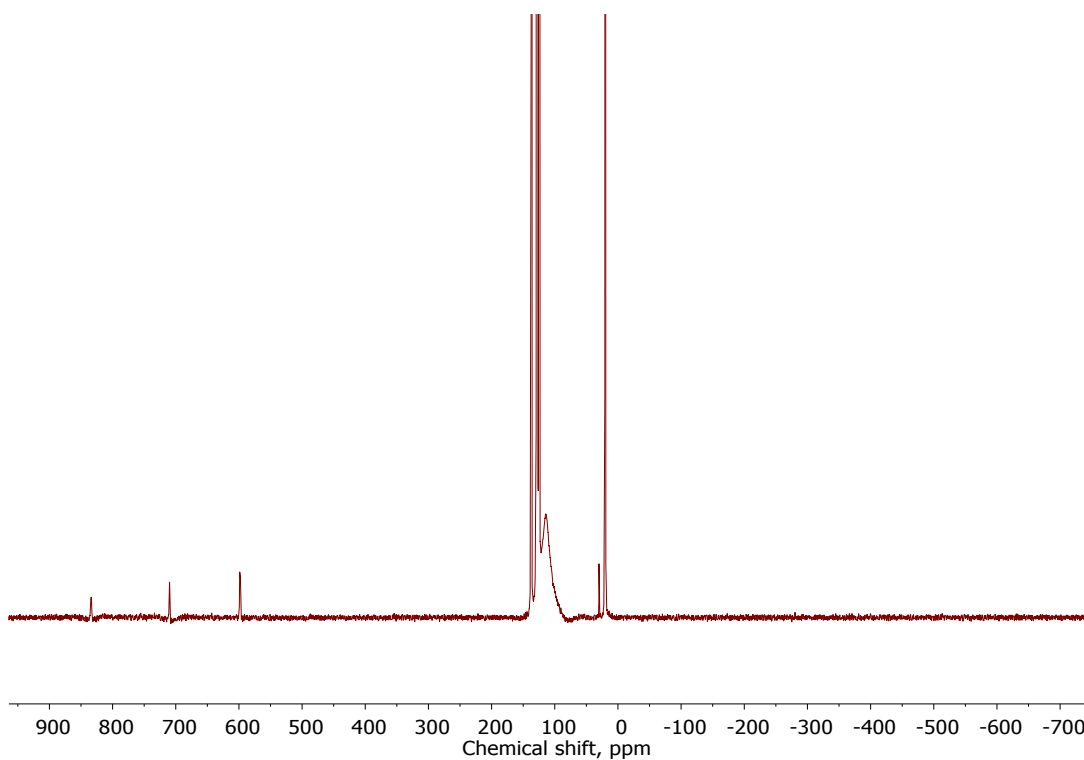
Figure S2. $^{13}C\{^1H\}$ NMR spectrum of **CoTp₂** in d$_8$-toluene (150.94 MHz, 293 K).
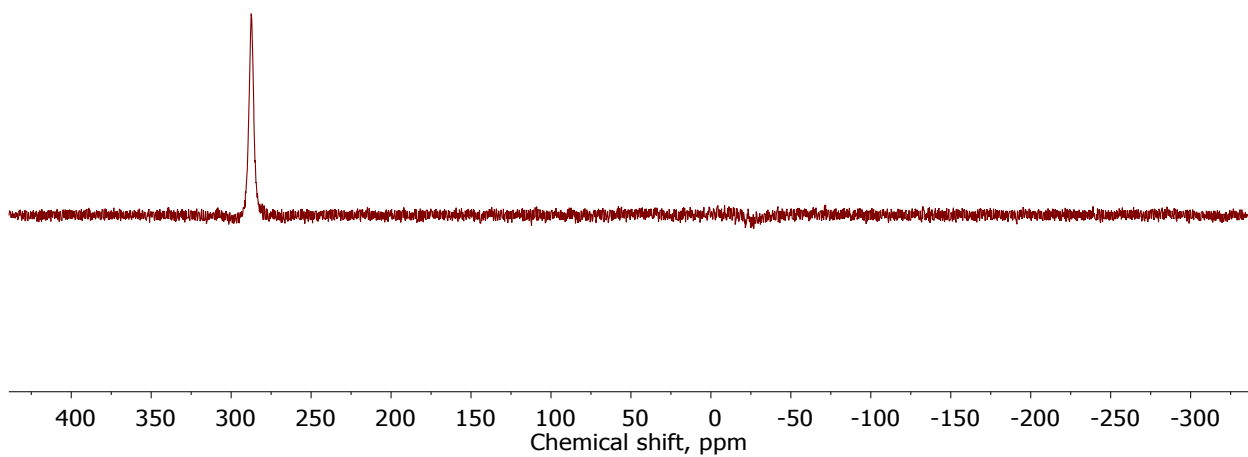
Figure S3. $^{11}B\{^{1}H\}$ NMR spectrum of **CoTp$_2$** in d$_8$-toluene (128 MHz, 293 K).
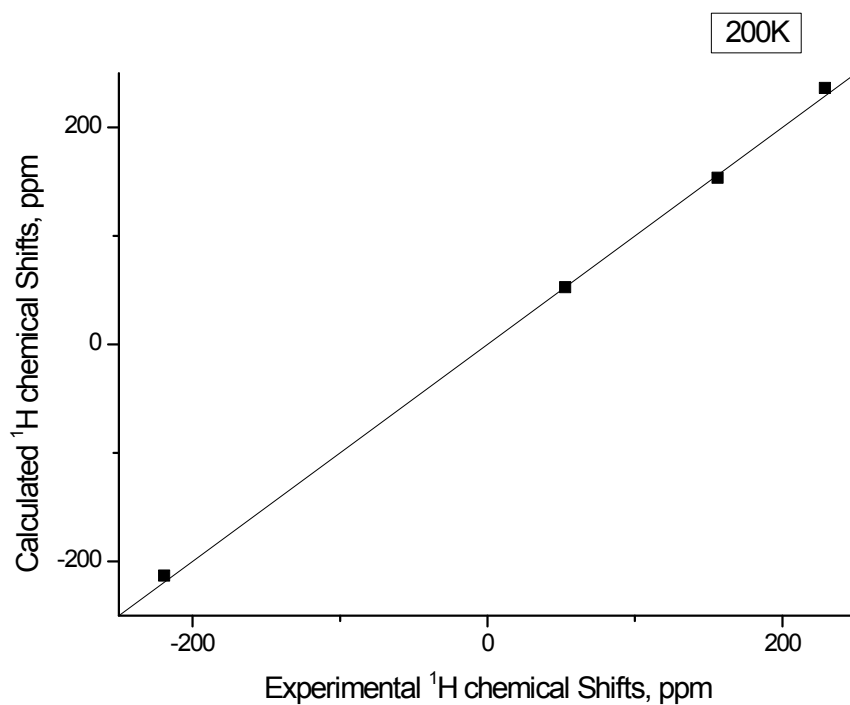
Figure S4. Calculated vs experimental chemical shifts in the ^{1}H NMR spectra for **CoTp$_2$** in d$_8$-toluene collected at 200 K.
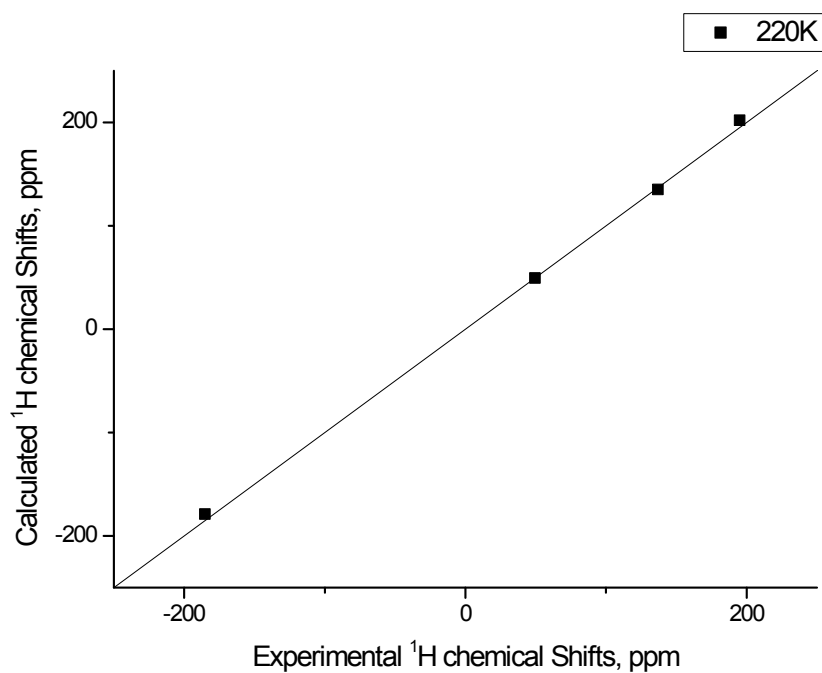
Figure S5. Calculated vs experimental chemical shifts in the ^{1}H NMR spectra for **CoTp$_2$** in d$_8$-toluene collected at 220 K.
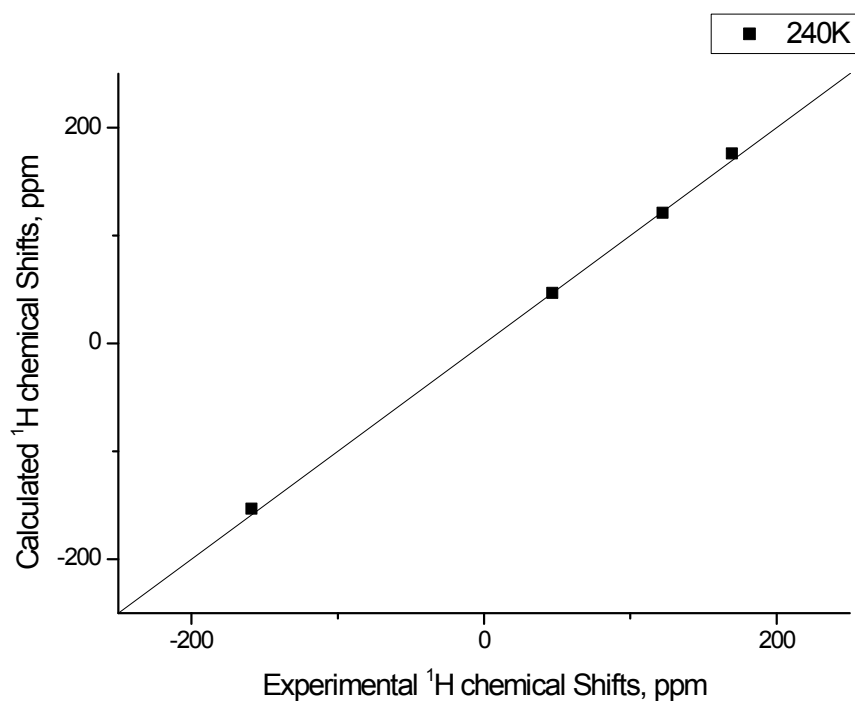
Figure S6. Calculated vs experimental chemical shifts in the ^{1}H NMR spectra for **CoTp$_2$** in d$_8$-toluene collected at 240 K.
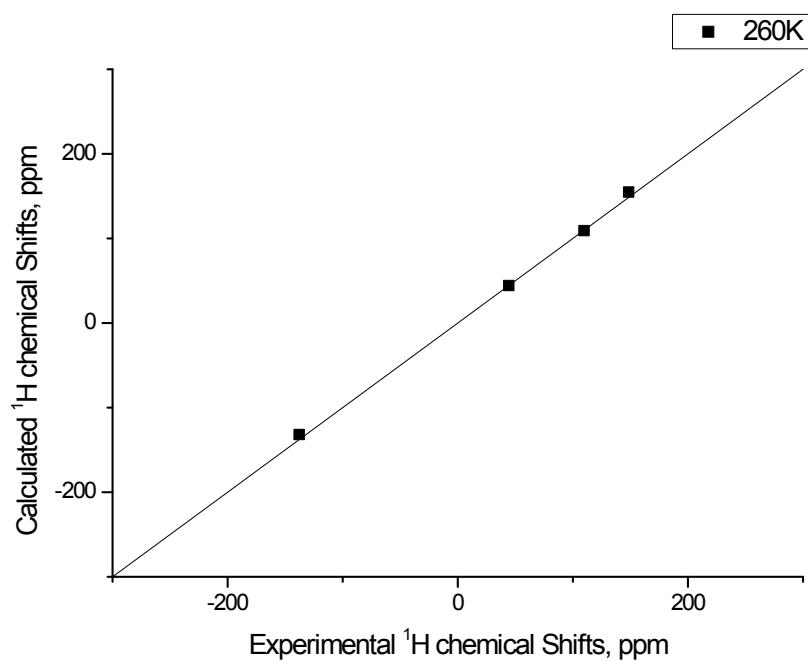
Figure S7. Calculated vs experimental chemical shifts in the ^{1}H NMR spectra for **CoTp$_2$** in d$_8$-toluene collected at 260 K.
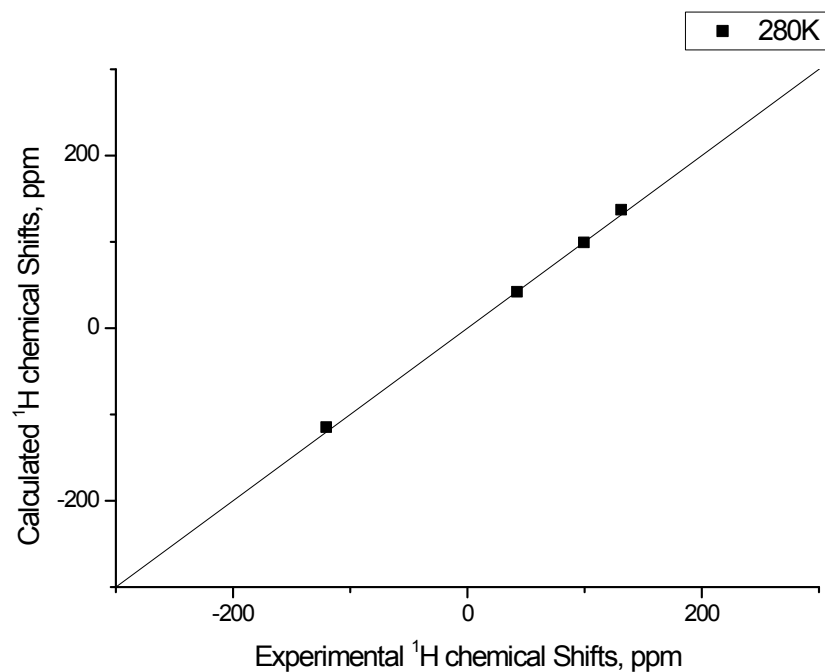
Figure S8. Calculated vs experimental chemical shifts in the ^{1}H NMR spectra for **CoTp$_2$** in d$_8$-toluene collected at 280 K.
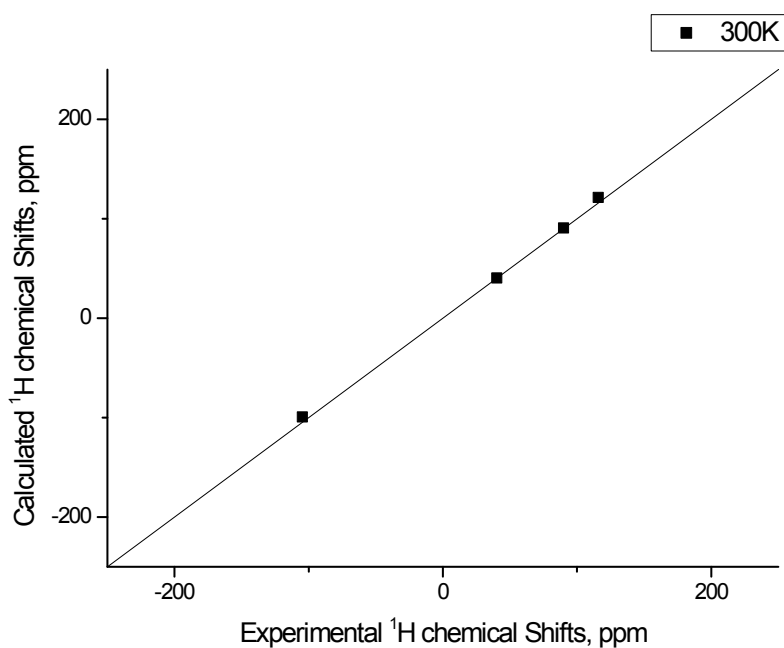
Figure S9. Calculated vs experimental chemical shifts in the ^{1}H NMR spectra for **CoTp$_2$** in d$_8$-toluene collected at 300 K.
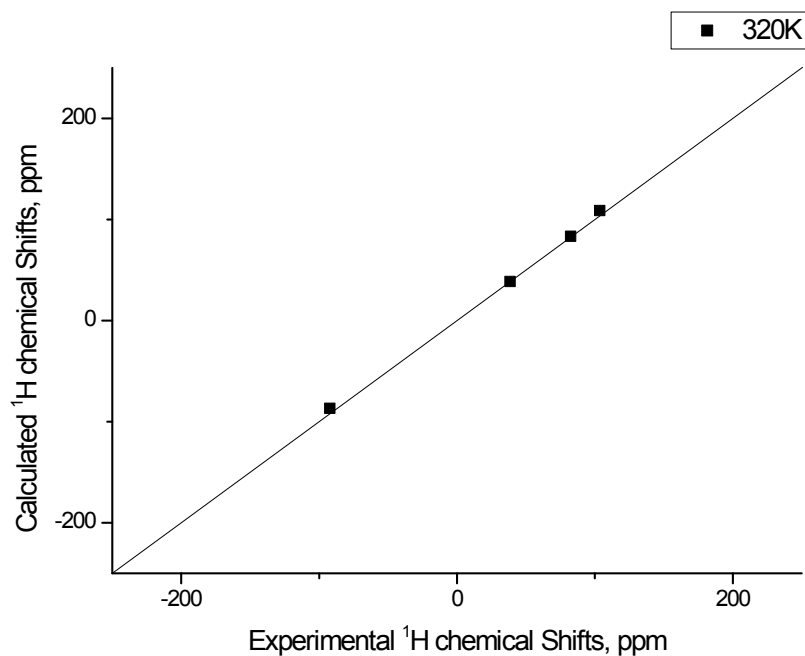
Figure S10. Calculated vs experimental chemical shifts in the ^{1}H NMR spectra for **CoTp$_2$** in d$_8$-toluene collected at 320 K.
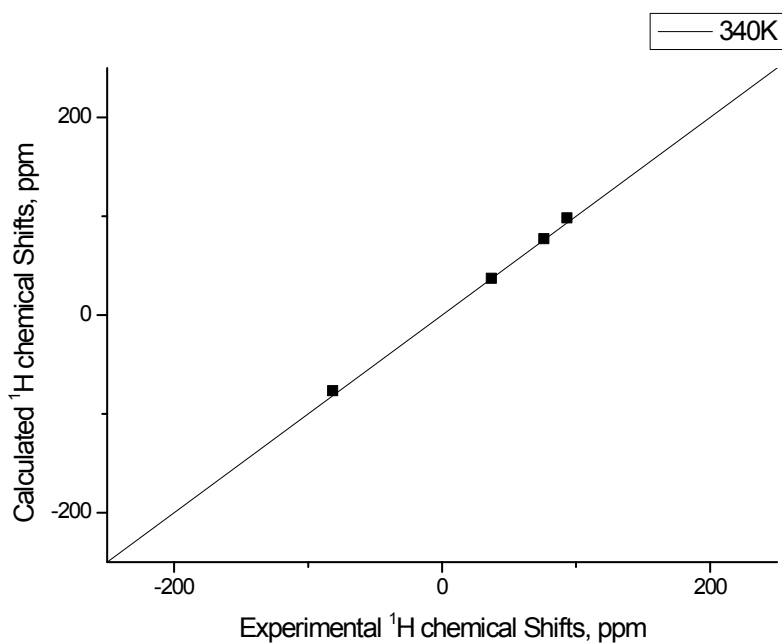
Figure S11. Calculated vs experimental chemical shifts in the ^{1}H NMR spectra for **CoTp$_2$** in d$_8$-toluene collected at 340 K.
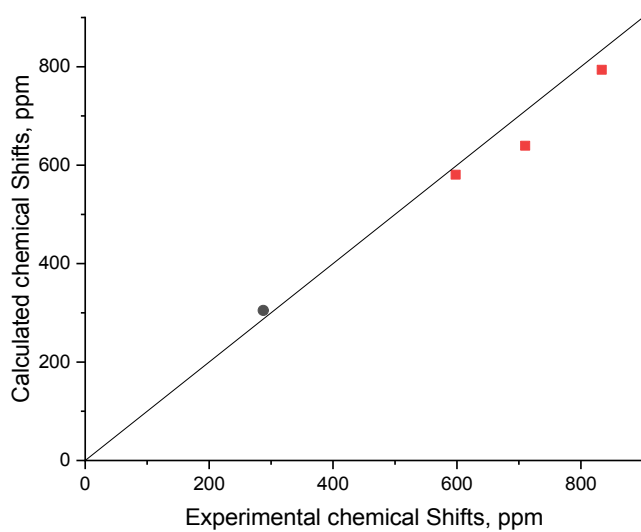
Figure S12. Calculated vs experimental chemical shifts in the ^{11}B (gray circle) and ^{13}C (red squares) NMR spectra for **CoTp$_2$** in d$_8$-toluene collected at 293 K. The straight line represents graphic of function $y = x$.
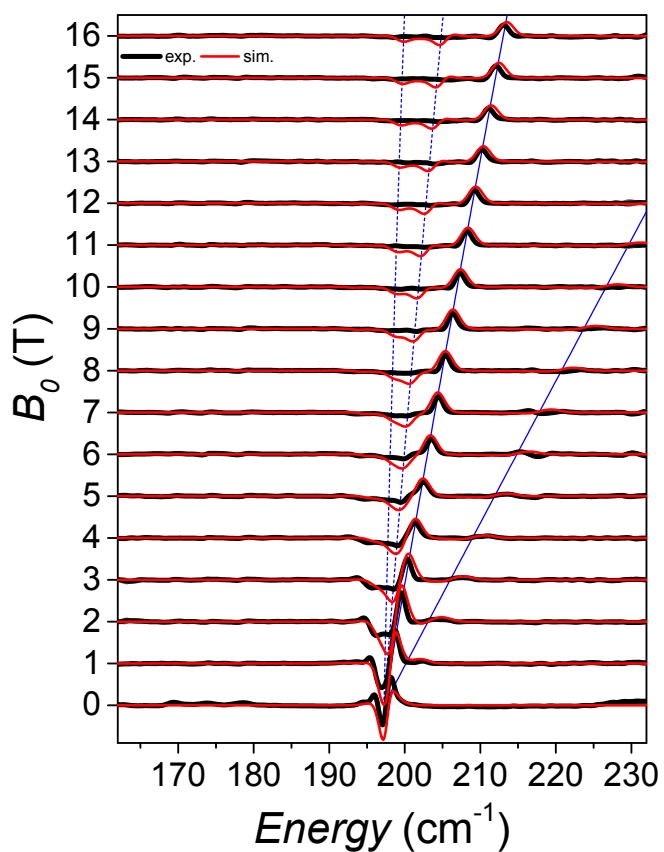
Figure S13. THz-EPR spectra simulations with the Hamiltonian (6) using parameters obtained from fitting the NMR data: $\lambda = 147.3$ cm^{-1}, $\sigma = 1.350$ and $\Delta = -632$ cm^{-1}.
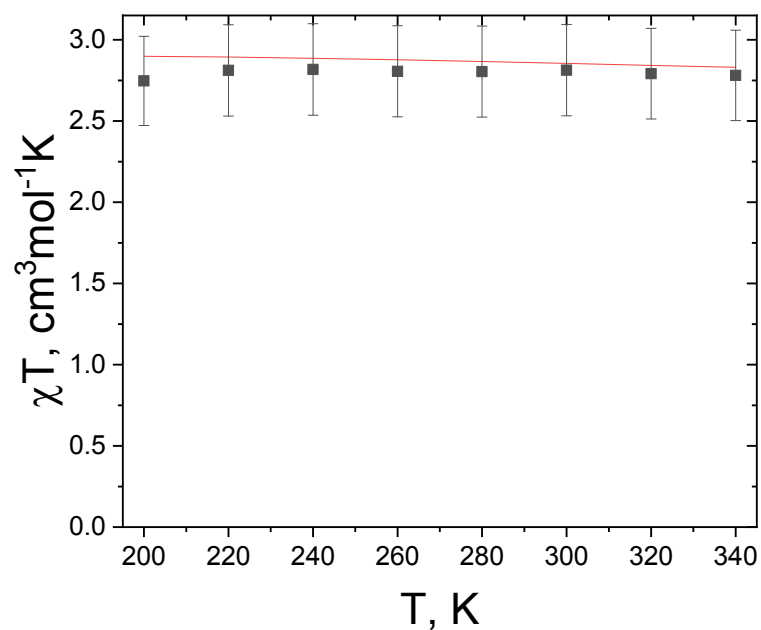
Figure S14. Magnetic susceptibility temperature dependence in solution for **CoTp$_2$** measured by the Evans method. [14, 15] The solid line shows the simulation using following parameters obtained from the NMR data fitting: values $\lambda = 147.3$ cm^{-1}, $\sigma = 1.350$ and $\Delta = -632$ cm^{-1}. The common 10 % measurement error of the Evans method is included.
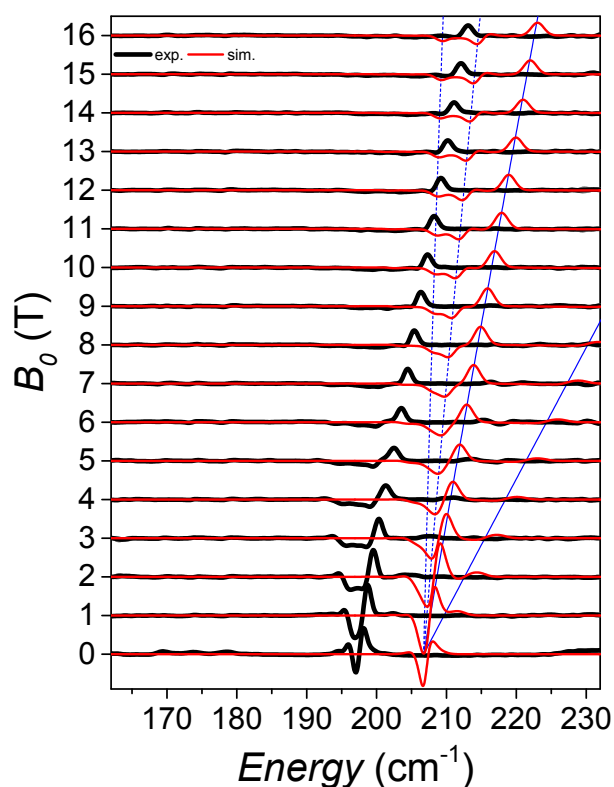
Figure S15. THz-EPR spectra simulations with the Hamiltonian (6) using paramters based on previously published energy scheme: $\lambda = 152.4$ cm^{-1}, $\sigma = 1.366$ and $\Delta = -632$ cm^{-1}.
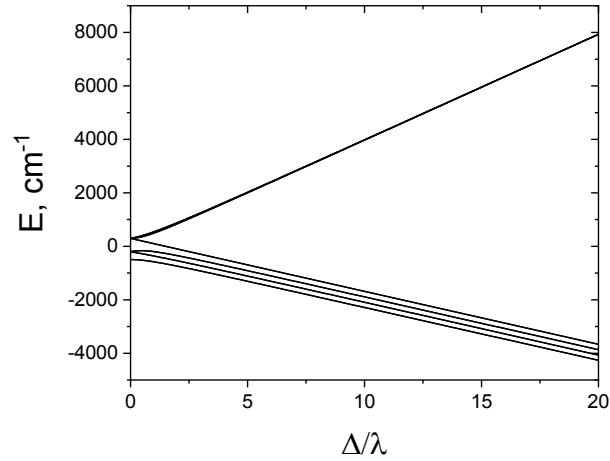
Figure S16. Energy levels in **CoTp$_2$** obtained by a numerical diagonalization of the Hamiltonian (**6**) with no magnetic field applied. The parameters used are σ = 1.350 and λ = 147.3 cm^{-1}.
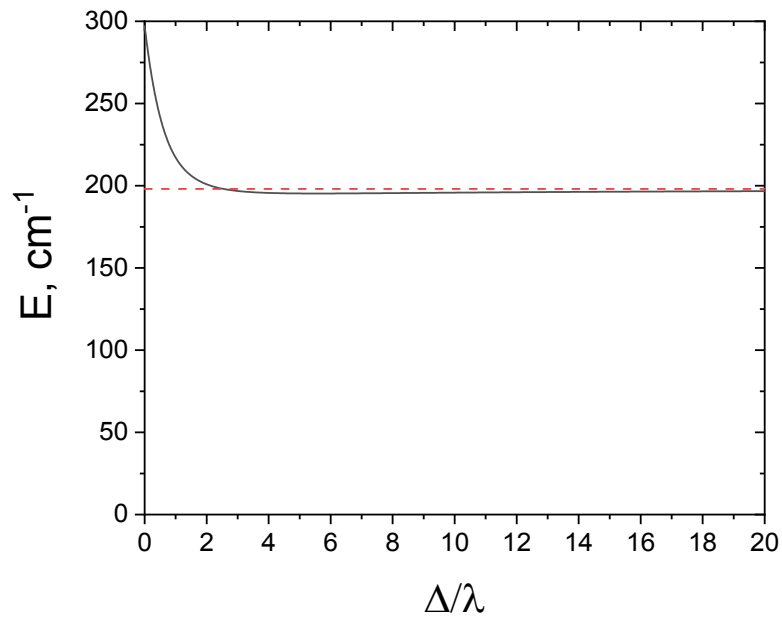
Figure S17. Energy of the 2nd KD in **CoTp$_2$** obtained by a numerical diagonalization of the Hamiltonian (6) with no magnetic field applied. The parameters used are σ = 1.350 and λ = 147.3 cm^{-1}. A red dashed line shows the value $\sigma\cdot\lambda$.

$$
\begin{pmatrix}
\Delta+\frac{3}{2}\sigma\lambda & 0 & 0 & & & & & & \\
0 & -2\Delta & \sqrt{\frac{3}{2}}\sigma\lambda & & 0 & & & & \\
0 & \sqrt{\frac{3}{2}}\sigma\lambda & \Delta+\frac{1}{2}\sigma\lambda & & & & & & \\
& & & \Delta-\frac{3}{2}\sigma\lambda & \sqrt{\frac{3}{2}}\sigma\lambda & 0 & & & \\
& 0 & & \sqrt{\frac{3}{2}}\sigma\lambda & -2\Delta & \sqrt{2}\sigma\lambda & & 0 & \\
& & & 0 & \sqrt{2}\sigma\lambda & \Delta-\frac{1}{2}\sigma\lambda & & & \\
& & & & & \Delta-\frac{1}{2}\sigma\lambda & \sqrt{2}\sigma\lambda & 0 & \\
& & & & & \sqrt{2}\sigma\lambda & -2\Delta & \sqrt{\frac{3}{2}}\sigma\lambda & 0 \\
& & 0 & & & 0 & \sqrt{\frac{3}{2}}\sigma\lambda & \Delta-\frac{3}{2}\sigma\lambda & \\
& & & & & & & \Delta+\frac{1}{2}\sigma\lambda & \sqrt{\frac{3}{2}}\sigma\lambda & 0 \\
& & & & & & 0 & \sqrt{\frac{3}{2}}\sigma\lambda & -2\Delta & 0 \\
& & & & & & 0 & 0 & \Delta+\frac{3}{2}\sigma\lambda
\end{pmatrix}
$$

Scheme S1. Symbolic form of the Hamiltonian (**6**) for S = 3/2 and L =1 with no magnetic field applied.

Table S1. The parameter values and the resulting energies of KDs (E_n) obtained by the simultaneous fitting of NMR and THz-EPR data for **CoTp₂** within the Hamiltonian (**6**).

λ, cm^{-1}	147.3
σ	1.350
Δ, cm^{-1}	632
E_1, cm^{-1}	0 (as set)
E_2, cm^{-1}	197
E_3, cm^{-1}	397
E_4, cm^{-1}	628
E_5, cm^{-1}	2255
E_6, cm^{-1}	2287

5. Supplementary references

1.   S. Trofimenko, *Journal of the American Chemical Society*, 1967, **89**, 3170-3177.

2.   E. Craven, E. Mutlu, D. Lundberg, S. Temizdemir, S. Dechert, H. Brombacher and C. Janiak, *Polyhedron*, 2002, **21**, 553-562.

3.   W. K. Myers, E. N. Duesler and D. L. Tierney, *Inorganic chemistry*, 2008, **47**, 6701-6710.

4.   F. Neese, *Wiley Interdisciplinary Reviews: Computational Molecular Science*, 2012, **2**, 73-78.

5.   J. Zhang, J. Li, L. Yang, C. Yuan, Y.-Q. Zhang and Y. Song, *Inorganic chemistry*, 2018, **57**, 3903-3912.

6.   C. van Wüllen, *The Journal of chemical physics*, 1998, **109**, 392-399.

7.   S. Grimme, J. Antony, S. Ehrlich and H. Krieg, *The Journal of chemical physics*, 2010, **132**, 154104.

8.   D. A. Pantazis, X.-Y. Chen, C. R. Landis and F. Neese, *Journal of chemical theory and computation*, 2008, **4**, 908-919.

9.   F. Weigend and R. Ahlrichs, *Physical Chemistry Chemical Physics*, 2005, **7**, 3297-3305.

10.   M. Kaupp and V. G. Malkin, *Calculation of NMR and EPR parameters: theory and applications*, John Wiley & Sons2006.

11.   A. M. Santos, F. E. Kühn, K. Bruus-Jensen, I. Lucas, C. C. Romão and E. Herdtweck, *Journal of the Chemical Society, Dalton Transactions*, 2001, 1332-1337.

12.   U. E. Bucher, A. Currao, R. Nesper, H. Rueegger, L. M. Venanzi and E. Younger, *Inorganic Chemistry*, 1995, **34**, 66-74.

13.   J. Ludwig, Y. B. Vasilyev, N. Mikhailov, J. Poumirol, Z. Jiang, O. Vafek and D. Smirnov, *Physical Review B*, 2014, **89**, 241406.

14.   D. Evans, *Journal of the Chemical Society (Resumed)*, 1959, 2003-2005.

15.   C. Piguet, *Journal of chemical education*, 1997, **74**, 815.